Supplemental Material for "Squeezing and Quantum State Engineering with Josephson Travelling Wave Amplifiers"

Arne L. Grimsmo[1], Alexandre Blais[1,2]

December 11, 2016

[1] *Institut quantique and Départment de Physique, Université de Sherbrooke, Sherbrooke, Québec, Canada J1K 2R1*
[2] *Canadian Institute for Advanced Research, Toronto, Canada*

Supplementary Method 1: Hamiltonian Treatment of a Josephson Traveling Wave Amplifier

In this Supplementary Note we give a more detailed Hamiltonian treatment of the Josephson Traveling Wave Amplifier (JTWPA) studied in the main text. The device we consider consists of N coupled Josephson junctions, as illustrated in Fig. 1 of the paper. Each junction has Josephson energy E_J, junction capacitance C_J, and is coupled to ground by an impedance $Z(\omega)$, describing a reactive and dissipationless element. We first treat the case of a single capacitance to ground, $Z(\omega) = 1/i\omega C$, before considering the more general case where the impedance contains resonances.

Without Resonances

We write the Lagrangian of the JTWPA in terms of the node fluxes, ϕ_n, following the standard lumped element approach,[1]

$$L = \sum_{n=0}^{N-1} \left\{ \frac{C}{2}\dot{\phi}_n^2 + \frac{C_J}{2}\Delta\dot{\phi}_n^2 - \frac{E_J}{2}\left(\frac{2\pi}{\Phi_0}\right)^2 \Delta\phi_n^2 + \frac{E_J}{4!}\left(\frac{2\pi}{\Phi_0}\right)^4 \Delta\phi_n^4 \right\}, \tag{1}$$

where $\Delta\phi_n = \phi_{n+1} - \phi_n$, $\Phi_0 = h/2e$ is the magnetic flux quantum, and we have expanded the Josephson junction cosine potential to fourth order.

In experimental realizations, the number of junctions is of the order of a few thousand, and the unit cell distance, a, is much smaller than the relevant microwave wavelengths. This justifies a continuum limit treatment of the device. Taking

$$x_n = na, \tag{2a}$$

$$\phi_n(t) \to \phi(x_n, t), \tag{2b}$$

$$\Delta\phi_n \to a\partial_x\phi(x_n, t), \tag{2c}$$

and defining continuum parameters through the relations

$$C = ca, \tag{3a}$$

$$E_J\left(\frac{2\pi}{\Phi_0}\right)^2 = \frac{1}{la}, \tag{3b}$$

$$C_J = \frac{1}{\omega_P^2 la}, \tag{3c}$$

$$\frac{E_J}{12}\left(\frac{2\pi}{\Phi_0}\right)^4 = \frac{\gamma}{a^3}, \tag{3d}$$

where $\omega_P = (2\pi/\Phi_0)\sqrt{E_J/C_J}$ is the junctions' plasma frequency, we can formally take the continuum limit $N \to \infty$, $a \to 0$ such that the length of the device $Na \equiv z$ is kept constant. A continuum Lagrangian can then be introduced

$$L[\phi, \partial_t\phi] = \frac{1}{2}\int_{-\infty}^{\infty} dx \bigg\{ c(x)[\partial_t\phi(x,t)]^2 - \frac{1}{l(x)}[\partial_x\phi(x,t)]^2 + \frac{1}{\omega_P^2(x)l(x)}[\partial_x\partial_t\phi(x,t)]^2 \\ + \gamma(x)[\partial_x\phi(x,t)]^4 \bigg\}. \tag{4}$$

The x-dependent parameters in the above expression are defined such that they take the values in Eq. (3) for $0 < x < z$, while outside this region we take $c(x) = c_0$, $l(x) = l_0$, $\omega_P(x) = \infty$ and $\gamma = 0$. Eq. (4) thus represents a JTWPA section extending from $x = 0$ to $x = z$, sandwiched between two identical semi-infinite linear transmission line sections extending from $x = -\infty$ to $x = 0$ and $x = z$ to $x = \infty$, respectively. We furthermore assume that the sections are impedance matched, $Z_0 = \sqrt{l_0/c_0} = \sqrt{l/c}$.

The Euler-Lagrange equation found from Eq. (4) is

$$\left(c\partial_t^2 - \frac{1}{l}\partial_x^2 - \frac{1}{\omega_P^2 l}\partial_x^2\partial_t^2\right)\phi = 2\gamma\partial_x[\partial_x\phi]^3, \tag{5}$$

where we have left out the x and t dependence of the fields and the parameters for notational simplicity. It is useful to find stationary solutions of the form $\phi(x,t) = \phi(x)e^{-i\omega t}$ to the linear part of Eq. (5), *i.e.*, the left hand side only of this equation. These classical solutions serve to determine the spatial dependence of the field in the absence of nonlinearity and are useful for constructing quantized solutions to the full problem.[2] We find that solutions of the form $\phi(x,t) = Ae^{-i\omega t + ik_\omega x}$ satisfies the linear part of Eq. (5) with a dispersion relation

$$k_\omega^2 = \frac{\omega^2}{v_1^2}\frac{1}{1-\omega^2/\omega_P^2} \qquad \text{for } 0 < x < z, \tag{6a}$$

$$k_\omega^2 = \frac{\omega^2}{v_0^2} \qquad \text{otherwise}, \tag{6b}$$

where $v_1 = 1/\sqrt{cl}$ and $v_0 = 1/\sqrt{c_0 l_0}$. Of course, the right hand side of Eq. (6a) has to be positive for travelling wave solutions to exist. In practice, we are interested in frequencies $\omega^2 \ll \omega_P^2$, such that the dispersion due to the junctions' plasma oscillations is relatively small.

We now wish to transform to a Hamiltonian. The canonical momentum to $\phi(x,t)$ is found from Eq. (4) in the usual way,

$$\pi = \frac{\delta L}{\delta[\partial_t\phi]} = \frac{\partial\mathcal{L}}{\partial[\partial_t\phi]} - \partial_x\frac{\partial\mathcal{L}}{\partial[\partial_x\partial_t\phi]} = c\partial_t\phi - \frac{1}{\omega_P^2 l}\partial_x^2\partial_t\phi, \tag{7}$$

where $\mathcal{L}$ is the Lagrangian density. Note that this differs from the usual prescription, $\pi = \partial\mathcal{L}/\partial(\partial_t\phi)$, due to the term proportional to $1/\omega_P^2$.[3] From this we can define a Hamiltonian $H = H[\phi, \pi]$,

$$H = \int_{-\infty}^{\infty} dx\pi\partial_t\phi - L, \tag{8}$$

which after an integration by parts and dropping a boundary term reads $H = H_0 + H_1$ with

$$H_0 = \frac{1}{2}\int_{-\infty}^{\infty} dx \bigg\{ c[\partial_t\phi]^2 + \frac{1}{l}[\partial_x\phi]^2 + \frac{1}{\omega_P^2 l}[\partial_x\partial_t\phi]^2 \bigg\}, \tag{9}$$

and

$$H_1 = -\frac{\gamma}{2}\int_0^z dx[\partial_x\phi]^4. \tag{10}$$

Note that although we express the Hamiltonian density in terms of $\partial_t\phi$ at this stage, this should be considered a function of π.

Quantization follows by the usual prescription of promoting the fields to operators $\phi(x,t) \to \hat{\phi}(x,t)$, $\pi(x,t) \to \hat{\pi}(x,t)$ and imposing the canonical commutation relation

$$[\hat{\phi}(x,t), \hat{\pi}(x',t)] = i\hbar\delta(x - x'). \tag{11}$$

We attack the problem by first considering only the linear Hamiltonian H_0, and diagonalizing this part by expanding $\hat{\phi}(x,t)$ in a set of mode functions and inserting into the Hamiltonian, not taking the interaction H_1 into account for the moment. We will subsequently use these modes to construct the full-nonlinear Hamiltonian.

We follow closely the treatment of a dielectric with an interface given by Santos and Loudon in Ref. 4 and expand the flux

$$\hat{\phi}(x,t) = \sum_{\nu=\mathrm{L,R}} \int_0^\infty d\omega \sqrt{\frac{\hbar}{2c(x)\omega}} g_{\nu\omega}(x) \hat{a}_{\nu\omega} e^{-i\omega t} + \mathrm{H.c.}, \tag{12}$$

where $[\hat{a}_{\nu\omega}, \hat{a}^\dagger_{\mu\omega'}] = \delta_{\nu\mu}\delta(\omega-\omega')$, and mode functions

$$g_{\nu\omega}(x) = \sqrt{\frac{1}{2\pi\eta_\omega(x)v(x)}} e^{\pm ik_\omega(x)x}, \tag{13}$$

where the $+$ sign is for $\nu = \mathrm{R}$ and the $-$ sign is for $\nu = \mathrm{L}$, with $k_\omega(x) = \eta_\omega(x)\omega/v(x)$ the wavevector. The refractive index, $\eta_\omega(x)$, has a different value inside and outside the JTWPA section, according to Eq. (6). We, however, neglect any reflections at the interfaces. More general expressions for the modefunctions that account for reflection can be fond in Ref. 4. Note that the refractive index should be real and symmetric, as we are not including absorption in the theory.

Using Eqs. (7) and (12) this gives for the canonical momentum $\hat{\pi}(x,t)$,

$$\hat{\pi}(x,t) = -i \sum_{\nu=\mathrm{L,R}} \int_0^\infty d\omega \sqrt{\frac{\hbar c(x)\omega}{2}} \varepsilon_\omega(x) g_{\nu\omega}(x) \hat{a}_{\nu\omega} e^{-i\omega t} + \mathrm{H.c.}, \tag{14}$$

where we have defined the dielectric function

$$\varepsilon_\omega(x) = 1 + \frac{\omega^2}{\omega_P^2(x)} \eta_\omega(x)^2. \tag{15}$$

Using Eq. (6) this can also be expressed as

$$\varepsilon_\omega(x) = \eta_\omega(x)^2 = \frac{1}{1-\omega^2/\omega_P^2}. \tag{16}$$

Note that the canonical commutation relation, Eq. (11), implies the following condition on the mode functions

$$\frac{1}{2}\sum_\nu \int_0^\infty d\omega \varepsilon_\omega(x) \left[g_{\nu\omega}(x') g^*_{\nu\omega}(x) + \mathrm{c.c}\right] = i\delta(x-x'). \tag{17}$$

This equality was proven to hold true for canonical fields of the form Eqs. (12) and (14) in Ref. 4 for real and symmetric $\eta_\omega(x)$ taking, as in Eq. (6), different constant values in different sections of a dielectric with interfaces. As was pointed out by these authors, however, the theory is not entirely satisfactory as travelling wave solutions do not exist for all frequencies. As a result the integration over all frequencies is not strictly valid.[4] A more careful analysis has to take absorption into account leading to localized excitations of the junction degrees of freedom.

Using the mode decomposition of $\hat{\phi}(x,t)$ and $\hat{\pi}(x,t)$, we can diagonalize the linear Hamiltonian $\hat{H}_0$. This follows directly from the results from Ref. 4. To that end, we first note that from Eq. (9) we can write the differential equation

$$\begin{aligned}\frac{\partial \hat{H}_0}{\partial t} = \frac{1}{2}\int_{-\infty}^\infty dx \Big\{ & c\partial_t\hat{\phi}\,\partial_t^2\hat{\phi} + c\partial_t^2\hat{\phi}\,\partial_t\hat{\phi} \\ & + \frac{1}{\omega_P^2 l}\left[\partial_x\partial_t^2\hat{\phi}\,\partial_x\partial_t\hat{\phi} + \partial_x\partial_t\hat{\phi}\,\partial_x\partial_t^2\hat{\phi}\right] \\ & + \frac{1}{l}\partial_x\hat{\phi}\,\partial_x\partial_t\hat{\phi} + \frac{1}{l}\partial_x\partial_t\hat{\phi}\,\partial_x\hat{\phi}\Big\}.\end{aligned} \tag{18}$$

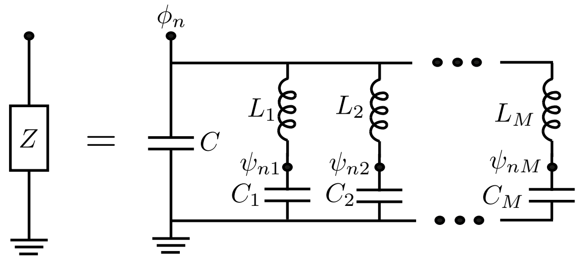

Figure 1: Representation of a general lossless admittance, $Z^{-1}(\omega)$, in terms of a set of modes, ψ_{nq}, with resonance frequencies $\omega_q = 1/\sqrt{L_q C_q}$. Note that we assume the presence of a zero-frequency component represented by the capacitance C.

After an integration by parts and dropping boundary terms, this reduces to

$$\frac{\partial \hat{H}_0}{\partial t} = \frac{1}{2}\int_{-\infty}^{\infty} dx \Big\{ \partial_t\hat{\phi}\,\partial_t\hat{\pi} + \partial_t\hat{\pi}\,\partial_t\hat{\phi} + \frac{1}{l}\partial_x\hat{\phi}\,\partial_x\partial_t\hat{\phi} + \frac{1}{l}\partial_x\partial_t\hat{\phi}\,\partial_x\hat{\phi} \Big\}, \tag{19}$$

which is exactly Equation (3.3) of Ref. 4 (with the identifications $\hat{E} \to -\partial_t\hat{\phi}$, $\hat{B} \to \partial_x\hat{\phi}$, $\hat{D} \to -\hat{\pi}$, $\mu_0 \to l$). It immediately follows from the results there [Eqs. (3.3) to (3.6)] that, after performing the integration over space, the linear Hamiltonian becomes

$$\hat{H}_0 = \sum_\nu \int_0^\infty d\omega \hbar\omega \hat{a}^\dagger_{\nu\omega}\hat{a}_{\nu\omega}, \tag{20}$$

where we have omitted the zero-point energy.

With Resonances

We now consider a general impedance $Z(\omega)$ describing a reactive, dissipationless element, coupling the node fluxes to ground in each unit cell, as illustrated in Fig. 1 of the paper. In general, we can represent this impedance with a circuit as illustrated in Fig. 1, and write for the inverse impedance (the admittance),[1,5]

$$Z^{-1}(\omega) = i\omega C + \sum_q \left(\frac{1}{i\omega C_q} + i\omega L_q\right)^{-1}, \tag{21}$$

where we include a zero-frequency component represented by the capacitance C. Following identical steps as before, the linear part of the continuum Lagrangian is now modified to

$$\begin{aligned} L_0 = \frac{1}{2}\int_{-\infty}^{\infty} dx \Big\{ & c[\partial_t\phi]^2 - \frac{1}{l}[\partial_x\phi]^2 + \frac{1}{\omega_P^2 l}[\partial_x\partial_t\phi]^2 \\ & + \sum_q \left[c_q[\partial_t\psi_q]^2 - \frac{1}{l_q}(\phi - \psi_q)^2 \right] \Big\}, \end{aligned} \tag{22}$$

where $c_q(x) = C_q/a$ and $l_q(x) = L_q a$ for $0 < x < z$ are the capacitance and inductance per unit cell associated to the q^{th} resonance, and $\psi_{nq}(t) \to \psi_q(x,t)$ is the continuum limit field for the resonance with frequency $\omega_q = 1/\sqrt{C_q L_q}$. We take $c_q(x) = 0$, $l_q(x) = \infty$ outside the JTWPA section. Similarly the linear Hamiltonian now reads after an integration by parts and dropping a boundary term

$$\begin{aligned} H_0 = \frac{1}{2}\int_{-\infty}^{\infty} dx \Big\{ & c[\partial_t\phi]^2 + \frac{1}{l}[\partial_x\phi]^2 + \frac{1}{\omega_P^2 l}[\partial_x\partial_t\phi]^2 \\ & + \sum_q \left[c_q[\partial_t\psi_q]^2 + \frac{1}{l_q}(\phi - \psi_q)^2 \right] \Big\}. \end{aligned} \tag{23}$$

The field $\psi_q(x,t)$ plays the role of a "matter field," with a single resonance at $\omega_q = 1/\sqrt{L_q C_q}$ coupling linearly to the "photonic field" $\phi(x,t)$. This type of light-matter coupling is a standard microscopic model, based on the Hopfield model,[6] for dispersion in linear media.[3,7,8]

The Euler-Lagrange equations for the fields are

$$\left(c\partial_t^2 - \frac{1}{l}\partial_x^2 - \frac{1}{\omega_P^2 l}\partial_x^2\partial_t^2\right)\phi = \sum_q \frac{1}{l_q}(\psi_q - \phi), \tag{24a}$$

$$c_q\partial_t^2\psi_q = \frac{1}{l_q}(\phi - \psi_q). \tag{24b}$$

As before we seek stationary solutions of the form $\phi(x,t) = Ae^{-i\omega t + ik_\omega x}$ and $\psi_q(x,t) = B_q e^{-i\omega t + ik_\omega x}$. The Euler-Lagrange equations can be used to find the dispersion relation of the medium, but also to relate the frequency components of the fields $\psi_q(x,t)$ to those of the field $\phi(x,t)$.[3] Indeed, solutions are found for Eq. (24) with

$$B_q = (1 - \omega^2/\omega_q^2)^{-1}A, \tag{25}$$

and

$$k_\omega^2 = \frac{\omega^2}{v_1^2}\frac{1 + \sum_q \frac{c_q/c}{1-\omega^2/\omega_q^2}}{1 - \omega^2/\omega_P^2} = \frac{-i\omega z^{-1}(\omega) l}{1 - \omega^2/\omega_P^2}, \tag{26}$$

inside the JTWPA section and $k_\omega^2 = \omega^2/v_0^2$ elsewhere, as before. $z^{-1}(\omega) = Z^{-1}(\omega)/a$ is here the admittance to ground per unit cell. Using Eq. (12) for $\phi(x,t)$ and Eq. (25) to relate the frequency components of the travelling wave solutions for the matter fields to those of the photonic field, we can write

$$\psi_q(x,t) = \sum_{\nu=\mathrm{L}}^{\mathrm{R}} \int_0^\infty d\omega \sqrt{\frac{\hbar}{2c(x)\omega}}\frac{1}{1-\omega^2/\omega_q^2(x)} g_{\nu\omega}(x) a_{\nu\omega} e^{-i\omega t} + \mathrm{H.c.} \tag{27}$$

Performing steps analogous to those in the previous section again leads to a diagonal linear Hamiltonian, H_0, as given in Eq. (20). First we find a differential equation for $\hat{H}_0$,

$$\begin{aligned}\frac{\partial H_0}{\partial t} = \frac{1}{2}\int_{-\infty}^{\infty} dx \Big\{ & c\partial_t\phi\,\partial_t^2\phi + c\partial_t^2\phi\,\partial_t\phi \\ & - \frac{1}{\omega_P^2 l}\left[\partial_x^2\partial_t^2\phi\,\partial_t\phi + \partial_t\phi\,\partial_x^2\partial_t^2\phi\right] \\ & + \frac{1}{l}\partial_x\phi\,\partial_x\partial_t\phi + \frac{1}{l}\partial_x\partial_t\phi\,\partial_x\phi \\ & + \sum_q \frac{1}{l_q}\Big[\partial_t\phi(\phi-\psi_q) + (\phi-\psi_q)\partial_t\phi\Big]\Big\},\end{aligned} \tag{28}$$

where we have used Eq. (24) and performed a partial integration, dropping a boundary term. This is of the same form as Eq. (19) if we define $\pi(x,t)$ as in Eq. (14) with a dielectric function

$$\varepsilon_\omega(x) = 1 + \frac{\omega^2}{\omega_P^2(x)}\eta_\omega(x)^2 + \sum_q \frac{c_q/c}{1-\omega^2/\omega_q^2}, \tag{29}$$

which from Eq. (26) reads

$$\varepsilon_\omega(x) = \eta_\omega(x)^2 = \frac{1 + \sum_q \frac{c_q/c}{1-\omega^2/\omega_q^2}}{1-\omega^2/\omega_P^2}. \tag{30}$$

With this, we can promote the fields to operators, and the canonical commutation relation as well as the diagonal form of $\hat{H}_0$ follows, again, from the results of Ref. 4.

Note that the numerator of the refractive index given by Eq. (30) has the standard form of a Sellmeir expansion that one expects for a dispersive medium with material resonances at ω_q.[3] The plasma oscillations of the junctions, however, play a somewhat different role from the "material" resonances due to the admittance $Z^{-1}(\omega)$. Indeed, a term of the type $(\partial_x\partial_t\phi)^2$, as appearing in our Hamiltonian, is used in macroscopic models for dispersive dielectrics.[3] It is therefore interesting to note that we here have two distinct types of dispersion present at the same time—a term $(\partial_x\partial_t\phi)^2$ in the Hamiltonian, stemming from junction plasma oscillations, *and* resonances associated to harmonic oscillators coupled linearly to the field $\hat{\phi}(x,t)$—and both effects arise from a microscopic theory in our case.

It is of course important to keep in mind that travelling wave solutions only exists for frequencies such that the right hand side of Eq. (26) is positive. Introducing resonances, as illustrated in Figure 3 of the main paper, introduces band gaps in the dispersion relation, as illustrated in Figure 2 of the paper. The theory developed here is valid away from any bandgap. A more general treatment would require keeping the "matter field" degrees of freedom and subsequently diagonalizing the linear Hamiltonian by introducing polariton fields.[7,8]

Nonlinear Hamiltonian

Having diagonalized the linear Hamiltonian H_0 we now consider the nonlinear contribution

$$\hat{H}_1 = -\frac{\gamma}{2}\int_0^z dx[\partial_x\hat{\phi}(x,t)]^4. \tag{31}$$

We use the expansion of $\hat{\phi}(x,t)$ in frequency modes $\hat{a}_{\nu\omega}$ introduced above, and assume that the fields $\hat{a}_{\nu\omega}$ are small except for close to the single pump frequency. More precisely, we assume a strong right moving, classical pump centered at a frequency Ω_p and corresponding wave number k_p, and take $\hat{a}_{R\omega} \to \hat{a}_{R\omega} + b(\omega)$, with $b(\omega)$ a c-number.

After dropping fast-rotating terms, the highly phase-mismatched left-moving field, and neglecting terms smaller than $\mathcal{O}[b(\omega)^2]$ we arrive at

$$\hat{H}_1 = \hat{H}_{\mathrm{CPM}} + \hat{H}_{\mathrm{SQ}} + H_{\mathrm{SPM}}, \tag{32}$$

where

$$\hat{H}_{\mathrm{CPM}} = -\frac{\hbar}{2\pi}\int_0^\infty d\omega d\omega' d\Omega d\Omega' \sqrt{k_\omega k_{\omega'}} \times \beta^*(\Omega)\beta(\Omega')\Phi(\omega,\omega',\Omega,\Omega')\hat{a}^\dagger_{R\omega}\hat{a}_{R\omega'} + \mathrm{H.c.}, \tag{33}$$

describing cross-phase modulation,

$$\hat{H}_{\mathrm{SQ}} = -\frac{\hbar}{4\pi}\int_0^\infty d\omega d\omega' d\Omega d\Omega' \sqrt{k_\omega k_{\omega'}}\beta(\Omega)\beta(\Omega')\Phi(\omega,\Omega,\omega',\Omega')\hat{a}^\dagger_{R\omega}\hat{a}^\dagger_{R\omega'} + \mathrm{H.c.}, \tag{34}$$

describing broadband squeezing, and

$$H_{\mathrm{SPM}} = -\frac{\hbar}{4\pi}\int_0^\infty d\omega d\omega' d\Omega d\Omega' \sqrt{k_\omega k_{\omega'}}\beta^*(\Omega)\beta(\Omega')\Phi(\omega,\omega',\Omega,\Omega')b^*(\omega)b(\omega') + \mathrm{H.c.}. \tag{35}$$

These equations are Eqs. (16)–(18) of the main paper. The dimensionless pump amplitude introduced here is defined as

$$\beta(\Omega) = \sqrt{3\gamma l}k_p B(\Omega), \tag{36}$$

where

$$B(\Omega) = \sqrt{\frac{\hbar Z_0}{4\pi\eta_\Omega\Omega}}b(\Omega). \tag{37}$$

and we drop the x-argument on variables when there is no danger of confusion, as $\gamma \neq 0$ only inside the JTWPA section. The dimensionless pump amplitude can also be written in terms of the ratio of the pump current to the Josephson junction critical current,

$$\beta(\Omega) = \frac{I_p(\Omega)}{4I_c}, \tag{38}$$

where $I_c = (2\pi/\Phi_0)E_J$ is the critical current, and we have related the pump amplitude to the pump current through $B(\Omega) = I_p(\Omega)Z_0/\Omega$ where $Z_0 = \sqrt{l/c}$ is the characteristic impedance.

As explained in the Methods section of the paper, by defining an interaction picture evolution operator and taking the initial and final times to minus and plus infinity respectively, we can define an asymptotic evolution operator (to first order in $\hat{H}_1$)

$$\hat{U} \equiv \hat{U}(-\infty,\infty) = e^{-\frac{i}{\hbar}\hat{K}_1}, \tag{39}$$

where

$$\hat{K}_1 = \hat{K}_{\text{CPM}} + \hat{K}_{\text{SQ}} + K_{SPM}. \tag{40}$$

The three Hamiltonian contributions are given by

$$\begin{aligned}\hat{K}_{\text{CPM}} = -\hbar\int_0^\infty & d\omega d\Omega d\Omega' \sqrt{k_\omega k_{\omega+\Omega-\Omega'}}\beta^*(\Omega)\beta(\Omega')\Phi(\omega,\omega+\Omega-\Omega',\Omega,\Omega')\hat{a}^\dagger_{R\omega}\hat{a}_{R(\omega+\Omega-\Omega')} \\ &+ \text{H.c.},\end{aligned} \tag{41}$$

which describes cross-phase modulation due to the pump,

$$\begin{aligned}\hat{K}_{\text{SQ}} = -\frac{\hbar}{2}\int_0^\infty & d\omega d\Omega d\Omega' \sqrt{k_\omega k_{\Omega+\Omega'-\omega}}\beta(\Omega)\beta(\Omega')\Phi(\omega,\Omega,\Omega+\Omega'-\omega,\Omega')\hat{a}^\dagger_{R\omega}\hat{a}^\dagger_{R(\Omega+\Omega'-\omega)} \\ &+ \text{H.c.},\end{aligned} \tag{42}$$

describing broadband squeezing, and

$$\begin{aligned}K_{\text{SPM}} = -\frac{\hbar}{2}\int_0^\infty & d\omega d\Omega d\Omega' \sqrt{k_\omega k_{\omega\Omega-\Omega'}}\beta^*(\Omega)\beta(\Omega')\Phi(\omega,\omega+\Omega-\Omega',\Omega,\Omega')b^*(\omega)b(\omega') \\ &+ \text{H.c.},\end{aligned} \tag{43}$$

describing pump self-phase modulation. Finally, taking the monochromatic pump limit, $b(\omega) \to b(\omega)\delta(\omega-\Omega_p)$, we arrive at Eqs. (24) and (25) of the main paper, while the classical pump Hamiltonian is simply $K_{SPM} = -\hbar z|\beta|^2 k_p b_p^* b_p$, where $\beta \equiv \beta(\Omega_p)$ and $b_p \equiv b(\Omega_p)$.

Asymptotic Input-Output Equations

We define Heisenberg picture asymptotic output fields $\hat{a}^{\text{out}}_{R\omega} = \hat{U}\hat{a}_{R\omega}\hat{U}^\dagger$, where $\hat{U}$ is defined in Eq. (39). To make a connection with the classical spatial equations of motion derived in Refs.[9–11] we note that $\hat{a}^{\text{out}}_{R\omega}$ is the solution to the following differential equation

$$\partial_z \hat{a}_{R\omega} = \frac{i}{\hbar}\left[\frac{d}{dz}\hat{K}_1, \hat{a}_{R\omega}\right] = 2i|\beta|^2 k_\omega \hat{a}_{R\omega} + i\lambda(\omega)e^{i\Delta k_L(\omega)z}\hat{a}^\dagger_{R(2\Omega_p-\omega)}, \tag{44}$$

where we recall that z is the length of the JTWPA section. The pump similarly is the solution to the classical equation of motion

$$\partial_z b_p = -\left\{\frac{d}{dz}K_{\text{SPM}}, b_p\right\} = i|\beta|^2 k_p b_p, \tag{45}$$

where $\{\,,\}$ denotes the Poisson bracket and we have neglected any back-action onto the pump from the quantized frequency components. Eqs. (44) and (45) are formally identical, up to a frequency-dependent normalization of the wave amplitudes, to the classical equations of motion derived in Refs.[9–11] With the anzats $\hat{a}_{R\omega}(z) = \tilde{a}_{R\omega}(z)e^{2i|\beta|^2 k_\omega z}$ and $b_p(z) = \tilde{b}_p(z)e^{i|\beta|^2 k_p z}$, we have the differential equations

$$\partial_z \tilde{a}_{R\omega} = i\lambda(\omega)e^{i\Delta k(\omega)z}\tilde{a}^\dagger_{R(2\Omega_p-\omega)}, \tag{46}$$

and $\partial_z \tilde{b}_p = 0$, where

$$\Delta k(\omega) = \Delta k_L(\omega) + 2|\beta|^2(k_p - k_{2\Omega_p-\omega} - k_\omega). \tag{47}$$

Eq. (46) can be solved exactly to give[10]

$$\tilde{a}_{R\omega}(z) = e^{i\Delta k(\omega)z/2}\Big[u(\omega,z)\tilde{a}_{R\omega}(0) + iv(\omega,z)\tilde{a}^\dagger_{R(2\Omega_p-\omega)}(0)\Big], \tag{48}$$

where

$$u(\omega,z)=\cosh[g(\omega)z]-\frac{i\Delta k(\omega)}{2g(\omega)}\sinh[g(\omega)z], \tag{49}$$

$$v(\omega,z)=\frac{\lambda(\omega)}{g(\omega)}\sinh[g(\omega)z], \tag{50}$$

$$g(\omega)=\sqrt{|\lambda(\omega)|^2-\left(\frac{\Delta k(\omega)}{2}\right)^2}. \tag{51}$$

This leads to the input-output relation Eq. (3) of the paper. A straightforward calculation shows that $|u(\omega,z)|^2-|v(\omega,z)|^2=1$, and that the modes satisfy the commutation relation

$$[\hat{a}^{\rm out}_{R\omega},\hat{a}^{\rm out\dagger}_{R\omega'}]=\delta(\omega-\omega'), \tag{52}$$

for any z, as they should.

From Eq. (48) it is straight forward to find the non-zero output field correlation functions for an incoming vacuum field,

$$\begin{aligned}\langle\hat{a}^{\rm out\dagger}_{R\omega}\hat{a}^{\rm out}_{R\omega'}\rangle &\equiv N_R(\omega,z)\delta(\omega-\omega')\\ &=|v(\omega,z)|^2\delta(\omega-\omega'),\end{aligned} \tag{53a}$$

$$\begin{aligned}\langle\hat{a}^{\rm out}_{R\omega}\hat{a}^{\rm out\dagger}_{R\omega'}\rangle &\equiv [N_R(\omega,z)+1]\delta(\omega-\omega')\\ &=|u(\omega,z)|^2\delta(\omega-\omega'),\end{aligned} \tag{53b}$$

$$\begin{aligned}&\langle\hat{a}^{\rm out}_{R\omega}\hat{a}^{\rm out}_{R\omega'}\rangle \equiv M(\omega,z)\delta(2\Omega_p-\omega-\omega')\\ &=iu(\omega,z)v(\omega,z)e^{i\Delta k(\omega)z}\delta(2\Omega_p-\omega-\omega'),\end{aligned} \tag{53c}$$

from which the squeezing spectrum can be computed easily.

The squeezing spectrum is typically probed in experiments by heterodyne measurement of filtered field quadratures.[12–15] We here give some more details on how the squeezing spectrum defined in Eq. (6) of the paper relates to such a measurement. We first define filtered output fields[12,16]

$$\hat{b}_{\omega_0}(t)=\int_{-\infty}^{\infty}d\omega f[\omega-\omega_0]e^{-i(\omega-\omega_0)t}\hat{a}^{\rm out}_{R\omega}, \tag{54}$$

where $f[\omega]$ satisfies $f[-\omega]=f^*[\omega]$ and refers to a narrowband low-pass filter capturing the experimental bandwidth.[17] We also define filtered quadratures $\hat{X}_{\omega_0}(t)=\hat{b}^\dagger_{\omega_0}(t)+\hat{b}_{\omega_0}(t)$, $\hat{Y}_{\omega_0}(t)=i\left[\hat{b}^\dagger_{\omega_0}(t)-\hat{b}_{\omega_0}(t)\right]$ and two-mode quadratures

$$\hat{U}^{\theta\pm}_{\omega_0}(t)=\frac{1}{\sqrt{2}}\left(\hat{Y}^\theta_{\omega_0}\pm\hat{Y}^\theta_{2\Omega_p-\omega_0}\right), \tag{55}$$

$$\hat{V}^{\theta\pm}_{\omega_0}(t)=\frac{1}{\sqrt{2}}\left(\hat{X}^\theta_{\omega_0}\pm\hat{X}^\theta_{2\Omega_p-\omega_0}\right). \tag{56}$$

Two-mode squeezing refers to the fluctuations in some of these two-mode quadratures being below the vacuum level. In the present case we find squeezing in the fluctuations

$$\Delta U^+_{\omega_0}=\overline{\langle\Delta\hat{U}^+_{\omega_0}(t)\Delta\hat{U}^+_{\omega_0}(t)\rangle}=\overline{\langle\Delta\hat{V}^-_{\omega_0}(t)\Delta\hat{V}^-_{\omega_0}(t)\rangle}, \tag{57}$$

where the overline denotes time-averaging. For a vacuum input field we find that the two-mode fluctuations are

$$\Delta U^+_{\omega_0}=\frac{1}{2}\int_0^\infty d\omega\Big\{|f[\omega-\omega_0]|^2S_R(\omega,z)+|f[2\Omega_p-\omega-\omega_0]|^2S_R(\omega,z), \tag{58}$$

giving a filtered version of the squeezing spectrum.

Supplementary Method 2: Squeezed Bath Engineering

In this appendix we derive a master equation for a collection of quantum systems interacting with multiple multimode squeezed baths, and give detailed results for the case of two qubits placed at the output of a JTWPA pumped by a single classical pump.

Master Equation for Multiple Systems and Multiple Squeezed Baths

We consider a number of quantum systems distributed along linear sections of a set of transmission lines. We label the transmission lines by the index i and the quantum systems coupled to the ith line by an index m_i. The systems couple to the transmission line voltages, $\hat{V}_i(x_i,t) = \partial_t\hat{\phi}_i(x_i,t)$, at some position x_i, via system operators $\hat{c}_{m_i}$. These system operators are furthermore assumed to rotate with frequencies ω_{m_i} in the interaction picture. The interaction Hamiltonian in the interaction picture is then of the form

$$\begin{aligned}\hat{H}_I(t) =& \hbar\sum_{i,m_i}\hat{B}_i(t)\sqrt{\frac{\kappa_{m_i}}{2\pi}}\left(\hat{c}_{m_i}e^{-i\omega_{m_i}t} + \text{H.c.}\right), && (59)\\ \hat{B}_i(t) =& i\int_0^\infty d\omega\left(\hat{b}^\dagger_{i\omega}e^{i\omega t} - \text{H.c.}\right), && (60)\end{aligned}$$

where $[\hat{b}_{i\omega},\hat{b}^\dagger_{j\omega'}] = \delta_{ij}\delta(\omega-\omega')$ are bath operators and κ_{m_i} describes the coupling strength of system m_i to the ith bath.

We do not consider a situation where the systems are cascaded,[18,19] *i.e.*, none of the systems are driven by the output of any of the other. The different baths can, however, be correlated, with a defining set of correlation functions

$$\langle\hat{b}^\dagger_{j\omega}\hat{b}_{i\omega'}\rangle = N_{ji}(\omega)\delta(\omega-\omega'), \tag{61a}$$

$$\langle\hat{b}_{j\omega}\hat{b}^\dagger_{i\omega'}\rangle = [N_{ji}(\omega)+1]\delta(\omega-\omega'), \tag{61b}$$

$$\langle\hat{b}_{j\omega}\hat{b}_{i\omega'}\rangle = \sum_k M^k_{ji}(\omega)\delta(\Omega_k-\omega-\omega'), \tag{61c}$$

where $N_{ji}(\omega) = N_{ij}(\omega)$ and $M^k_{ji}(\omega) = M^k_{ij}(\omega)$. This generalizes Eq. (53) and includes, for example, setups of the type illustrated in Figures 8 and 9 of the paper, where the output field of multiple JTWPAs are combined on beam splitters before being incident on the quantum systems.

Following the standard approach,[20] we find the following master equation for the reduced system density matrix under the usual Born-Markov approximation

$$\begin{aligned}\dot{\rho}(t) = \sum_{ij}\sum_{m_in_j}\frac{\sqrt{\kappa_{m_i}\kappa_{n_j}}}{2\pi}\Big\{& e^{-i(\omega_{m_i}-\omega_{n_j})t}S^-_{ji}(t,\omega_{n_j})\left(c_{m_i}\rho c^\dagger_{n_j} - \rho c^\dagger_{n_j}c_{m_i}\right)\\ &+ e^{i(\omega_{m_i}-\omega_{n_j})t}S^+_{ji}(t,\omega_{n_j})\left(c^\dagger_{m_i}\rho c_{n_j} - \rho c_{n_j}c^\dagger_{m_i}\right)\\ &+ e^{i(\omega_{m_i}+\omega_{n_j})t}S^-_{ji}(t,\omega_{n_j})\left(c^\dagger_{m_i}\rho c^\dagger_{n_j} - \rho c^\dagger_{n_j}c^\dagger_{m_i}\right)\\ &+ e^{-i(\omega_{m_i}+\omega_{n_j})t}S^+_{ji}(t,\omega_{n_j})\left(c_{m_i}\rho c_{n_j} - \rho c_{n_j}c_{m_i}\right) + \text{H.c.}\Big\},\end{aligned} \tag{62}$$

where we have defined bath correlation functions

$$S^\pm_{ji}(t,\omega) = \int_0^\infty d\tau e^{\pm i\omega\tau}\langle\hat{B}_j(t-\tau)\hat{B}_i(t)\rangle, \tag{63}$$

with $\omega > 0$ and the brackets refer to an expectation value with respect to the bath density matrix ρ_B. At this stage we can invoke a rotating wave approximation (RWA). For example, we can approximate

$$\begin{aligned}e^{i(\omega_m+\omega_n)t}S^-_{ji}(t,\omega_n) \simeq& -\int_0^\infty d\tau\int_{-\infty}^\infty d\omega d\omega' e^{-i(\omega_n-\omega)\tau}\langle\hat{b}_{j\omega}\hat{b}_{i\omega'}\rangle_B e^{i(\omega_m+\omega_n-\omega-\omega')t}\\ =& -\pi\sum_k M^k_{ij}(\omega_n)e^{i(\omega_m+\omega_n-2\Omega_k)t},\end{aligned} \tag{64}$$

where we have used

$$\int_0^\infty d\tau e^{i(\omega+\omega')\tau} = \pi\delta(\omega+\omega') + iP\left(\frac{1}{\omega+\omega'}\right), \tag{65}$$

and dropped the small principal part. We find similar expressions for the other terms in Eq. (62), leading to the interaction picture Master equation

$$\begin{aligned}\dot{\rho}(t) = \sum_{ijk}\sum_{m_i n_j} \frac{\sqrt{\kappa_{m_i}\kappa_{n_j}}}{2} \Big\{ & e^{-i(\omega_{m_i}-\omega_{n_j})t}[N_{ji}(\omega_{n_j})+1]\left(c_{m_i}\rho c_{n_j}^\dagger - \rho c_{n_j}^\dagger c_{m_i}\right) \\ & + e^{i(\omega_{m_i}-\omega_{n_j})t} N_{ji}(\omega_{n_j})\left(c_{m_i}^\dagger \rho c_{n_j} - \rho c_{n_j} c_{m_i}^\dagger\right) \\ & - e^{i(\omega_{m_i}+\omega_{n_j}-2\Omega_k)t} M_{ji}^k(\omega_{n_j})\left(c_{m_i}^\dagger \rho c_{n_j}^\dagger - \rho c_{n_j}^\dagger c_{m_i}^\dagger\right) \\ & - e^{-i(\omega_{m_i}+\omega_{n_j}-2\Omega_k)t} M_{ji}^{k*}(\omega_{n_j})\left(c_{m_i}\rho c_{n_j} - \rho c_{n_j} c_{m_i}\right) + \text{H.c.}\Big\}.\end{aligned} \tag{66}$$

Note that this master equation includes dissipative interactions between systems even if they are not coupled to the same bath, $i \neq j$, if the baths are correlated according to Eq. (61). As we will see in Supplementary Method 3, this is the type of interactions that give rise to the diagonal edges in the cluster state graphs considered there. But first, we focus in the next subsection on the simple case of two qubits coupled to the left- and right-moving fields of a single transmission line.

Two Qubits

In this section we consider two qubits coupled to the left- and right moving field of a transmission line (in general both fields can be squeezed). We take both fields to have correlation functions as in Eq. (53) without any cross correlations between the two fields ($N_{ji}, M_{ji} \propto \delta_{ji}$ in Eq. (61)).

The qubits have free Hamiltonians $\hat{H}_m = \omega_m \hat{\sigma}_z^{(m)}/2$, $m = 1, 2$, and we take $c_{m_i} \to \sigma_-^{(m)}$ in Eq. (66). We also assume that the qubits are off-resonant, $\omega_1 \neq \omega_2$. The resulting master equation is defined by the Lindbladian

$$\begin{aligned}\mathcal{L} = & \sum_{\substack{\nu=\text{L,R}\\ m=1,2}} \left\{\frac{\gamma_m}{2}(N_{m,\nu}+1)\mathcal{D}[\hat{\sigma}_-^{(m)}] + \frac{\gamma_m}{2} N_{m,\nu}\mathcal{D}[\hat{\sigma}_+^{(m)}]\right\} \\ & - \frac{\sqrt{\gamma_1\gamma_2}}{2}\left\{e^{i(\omega_1+\omega_2-2\Omega_\nu)t} M_\nu \mathcal{C}[\hat{\sigma}_+^{(1)}, \hat{\sigma}_+^{(2)}] + e^{-i(\omega_1+\omega_2-2\Omega_\nu)t} M_\nu^* \mathcal{C}[\hat{\sigma}_-^{(1)}, \hat{\sigma}_-^{(2)}]\right\},\end{aligned} \tag{67}$$

where we have dropped off-resonant terms rotating at $\omega_1 - \omega_2$, defined

$$\mathcal{C}[A, B]\rho = (A\rho B + B\rho A - \{AB, \rho\}), \tag{68}$$

and γ_m the decay rate of qubit m, which has contributions from both the left- and the right-moving field. The parameters $N_{m,\nu} = N_\nu(\omega_m)$ and $M_\nu = [M_\nu(\omega_1) + M_\nu(\omega_2)]/2$ are, respectively, thermal photon number and squeezing parameters for each field.

If the qubits are not tuned into resonance with the squeezing interaction induced by the pump fields, $\omega_1 + \omega_2 \not\simeq 2\Omega_\nu$, the last two lines of Eq. (67) can be dropped in an RWA. In this case, the two qubits are effectively interacting with independent thermal baths, and will reach an uncorrelated thermal steady state, $\rho_{\text{ss}} = \rho_1 \otimes \rho_2$, where

$$\rho_m = \begin{pmatrix} \frac{N_{m,\text{tot}}}{2N_{m,\text{tot}}+2} & 0 \\ 0 & \frac{N_{m,\text{tot}}+2}{2N_{m,\text{tot}}+2} \end{pmatrix}, \tag{69}$$

where $N_{m,\text{tot}} = N_{m,\text{R}} + N_{m,\text{L}}$ is the total thermal photon number at the frequency of qubit m. For a left moving field in the vacuum state, $N_{\text{L,m}} = 0$, this gives the atomic inversion quoted in the main paper.

As discussed in the paper, when the qubits are tuned into resonance with the squeezing interaction, they become entangled and encode information about the squeezing spectrum. This can be exploited to use the qubits as a spectroscopic probe. Assuming a left moving field in the vacuum state, and taking $\omega_1 + \omega_2 = 2\Omega_R$, Eq. (67) reduces to

$$\mathcal{L} = \sum_{m=1,2} \left\{ \frac{\gamma_m}{2}(N_m + 2)\mathcal{D}[\hat{\sigma}_-^{(m)}] + \frac{\gamma_m}{2} N_m \mathcal{D}[\hat{\sigma}_+^{(m)}] \right\} - \frac{\sqrt{\gamma_1\gamma_2}}{2}\mathcal{S}_{M_\mathrm{R}}[\hat{\sigma}_+^{(1)}, \hat{\sigma}_+^{(2)}], \tag{70}$$

where $N_m = N_{m,\mathrm{R}}$, $M = [M_\mathrm{R}(\omega_1) + M_\mathrm{R}(\omega_2)]/2$ and

$$\mathcal{S}_M[A,B]\rho = M\left(A\rho B + B\rho A - \{AB, \rho\}\right) + \mathrm{H.c.} \tag{71}$$

The steady state of Eq. (70) can be found analytically if we assume that the qubits start in the ground state. We find (in the basis $\{|ee\rangle, |eg\rangle, |ge\rangle, |gg\rangle\}$)

$$\rho_\mathrm{ss} = \begin{pmatrix} \frac{N_1N_2}{A} + C & 0 & 0 & \sqrt{\gamma_1\gamma_2}B\,M \\ 0 & \frac{N_1(N_2+2)}{A} - C & 0 & 0 \\ 0 & 0 & \frac{(N_1+2)N_2}{A} - C & 0 \\ \sqrt{\gamma_1\gamma_2}B\,M & 0 & 0 & \frac{(N_1+2)(N_2+2)}{A} + C \end{pmatrix}, \tag{72}$$

where

$$A = 4(N_1+1)(N_2+1), \tag{73a}$$
$$B = \gamma_1(N_1+1) + \gamma_2(N_2+2), \tag{73b}$$
$$C = \frac{1}{A}\frac{4\gamma_1\gamma_2|M|^2}{B^2 - 4\gamma_1\gamma_2|M|^2}. \tag{73c}$$

This gives steady state expectation values

$$\langle\hat{\sigma}_z^{(m)}\rangle = -\frac{1}{N_m+1}, \tag{74a}$$
$$\langle\hat{\sigma}_x^{(1)}\hat{\sigma}_x^{(2)}\rangle = -\langle\hat{\sigma}_y^{(1)}\hat{\sigma}_y^{(2)}\rangle = \frac{1}{A}\frac{2\sqrt{\gamma_1\gamma_2}\,\mathrm{Re}M}{B^2 - 4\gamma_1\gamma_2|M|^2}, \tag{74b}$$
$$\langle\hat{\sigma}_x^{(1)}\hat{\sigma}_y^{(2)}\rangle = -\frac{1}{A}\frac{2\sqrt{\gamma_1\gamma_2}\,\mathrm{Im}M}{B^2 - 4\gamma_1\gamma_2|M|^2}, \tag{74c}$$

from which both N_m and M_m, and thus the squeezing spectrum of the source, can be extracted. For the simplifying symmetric assumptions $\gamma_1 = \gamma_2 \equiv \gamma$ and $N_1 = N_2 \equiv N$, this leads to Eqs. (7) and (8) of the paper.

Another interesting case is when both the left- and right moving fields are squeezed or, equivalently, the qubit couples to a single squeezed field. This could be realized, *e.g.*, by ending the transmission line with a mirror as indicated in Figure 6 (c) of the paper. This gives higher degrees of entanglement between the qubits, as the vacuum noise of the left moving field otherwise reduces correlations between them. In particular, taking $N_{m,\nu} = N/2$, $M_\nu = M/2$ and $\gamma_1 = \gamma_2$ in Eq. (67), and furthermore assuming $|M| = \sqrt{N(N+1)}$, we find that the steady state is given by the pure state in Eq. (9) of the paper.

Supplementary Method 3: Generating cluster states

In this appendix we give more details regarding the dissipative generation of CV cluster states. Recall that the cluster state $|\phi_G\rangle$ with respect to a graph G is the unique pure state satisfying

$$\Big(\hat{y}_v - \sum_{w\in\mathcal{N}(v)} a_{vw}\hat{x}_w\Big)|\phi_G\rangle = 0 \quad \forall v \in V, \tag{75}$$

where $-1 \leq a_{vw} \leq 1$ is the weight of the (undirected) edge $\{v,w\}$ and $\mathcal{N}(v)$ denotes the neighborhood of v. We can define an adjacency matrix, $A = [a_{vw}]$ (with $a_{vw} = 0$ if there is no edge $\{v,w\}$ in the graph), and we use the graph G and its adjacency matrix A interchangeably when referring to the graph in the following.

The general question of dissipatively preparing pure Gaussian states was addressed by Koga and Yamamoto in Ref. 21 and, in particular, they found a Lindblad master equation $\dot{\rho} = \mathcal{L}_G(\varepsilon)\rho$ whose unique steady state approaces Eq. (75), in the limit of infinite squeezing. A Lindbladian that achieves this is

$$\mathcal{L}_G(\varepsilon)/\kappa = \sum_v \mathcal{D}[L_v(\varepsilon)], \tag{76}$$

where κ is a decay rate setting the overall time-scale and the Lindblad operators are

$$L_v(\varepsilon) = \hat{y}_v - \sum_{w\in\mathcal{N}(v)} a_{vw}\hat{x}_w - i\varepsilon\hat{x}_v. \tag{77}$$

The steady state approaches Eq. (75) in the limit $\varepsilon \to 0^+$.

In the special case of a bicolorable graph, meaning that every vertex can be given one out of two colors in such a way that every edge connects vertices of different colors, the Lindbladian Eq. (76) is to first order in ε

$$\begin{aligned}
\mathcal{L}_G(\varepsilon)/\kappa = \frac{1}{2}\sum_{v\in V}&\Big\{(1+D_v+2\varepsilon)\mathcal{D}[\hat{c}_v] \\
&+ (1+D_v-2\varepsilon)\mathcal{D}[\hat{c}_v^\dagger] + (D_v-1)\mathcal{S}_1[\hat{c}_v^\dagger,\hat{c}_v^\dagger]\Big\} \\
&- \sum_{\{v,w\}\in E} a_{vw}\mathcal{S}_i[\hat{c}_v^\dagger,\hat{c}_w^\dagger] \\
&+ \sum_{\{w,w'\}\in E_2} \frac{D_{w,w'}}{2}\Big\{\mathcal{S}_1[\hat{c}_w^\dagger,\hat{c}_{w'}^\dagger] + \mathcal{D}_1[\hat{c}_w,\hat{c}_{w'}]\Big\}.
\end{aligned} \tag{78}$$

Recall that E is the set of all pairs of vertices $\{v,w\}$ connected by an edge. Furthermore, we have defined E_2 as the set of all pairs of distinct vertices $\{w,w'\}$ such that there exists some $v \neq w, w'$ such that $w, w' \in \mathcal{N}(v)$. In other words, E_2 is the set of all next-nearest neighbors. Note that the sum over edges in E is a sum over *undirected* edges, *i.e.*, there is *one* term in the sum for every *pair* of vertices connected by an edge, and similarly for the sum over E_2. We have furthermore defined

$$D_v = \sum_{w\in\mathcal{N}(v)} a_{v,w}^2, \tag{79}$$

$$D_{w,w'} = \sum_{\substack{v \text{ s.t.} \\ w,w'\in\mathcal{N}(v)}} a_{v,w}a_{v,w'}. \tag{80}$$

The former can be recognized as the sum of the weights of all "2-paths" starting and ending at v, and the latter as the sum of the weights of all "2-paths" connecting the two vertices $\{w,w'\}$. The weight of a 2-path is here defined to be the product of the weights of the two respective edges.

Eq. (78) takes a particularly simple form if the following two geometric conditions for the graph G are satisfied:

1. The sum of all 2-paths starting and ending at the same vertex add up to one: $D_v = 1$.

2. The sum of all 2-paths connecting two different vertices cancel out: $D_{w,w'} = 0$.

Note that these two criteria are equivalent to saying that the adjacency matrix defining the graph is self-inverse, $A = A^{-1}$.[22] In this case,

$$\mathcal{L}_G(\varepsilon) = \sum_{v\in V}\Big\{\kappa(1+\varepsilon)\mathcal{D}[\hat{c}_v] + \kappa(1-\varepsilon)\mathcal{D}[\hat{c}_v^\dagger]\Big\} - \sum_{\{v,w\}\in E}\kappa a_{vw}\mathcal{S}_i[\hat{c}_v^\dagger,\hat{c}_w^\dagger]. \tag{81}$$

Or, by defining $|M| = 1/2\varepsilon$, and N through $|M| = \sqrt{N(N+1)}$ we can write to first order in ε

$$|M|\mathcal{L}_G(\varepsilon) = \sum_{v\in V}\Big\{\kappa(N+1)\mathcal{D}[\hat{c}_v] + \kappa N\mathcal{D}[\hat{c}_v^\dagger]\Big\} - \sum_{\{v,w\}\in E}\kappa|M|a_{vw}\mathcal{S}_i[\hat{c}_v^\dagger,\hat{c}_w^\dagger]. \tag{82}$$

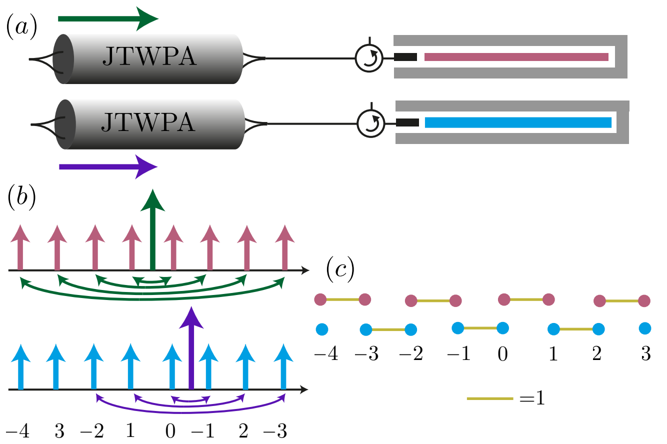

Figure 2: Independent broadband squeezing sources with a single pump frequency generates trivial cluster state graphs consisting of disjoint pairs of connected vertices. (a) Experimental setup with JTWPAs whose output fields are incident on independent resonators. (b) placement of pump frequencies with respect to the frequencies of the resonator modes. The numbers indicate the macronode index $\mathcal{M}$. Note that the two resonators have identical spectral profiles. (c) The graph generated by the dissipative interactions. To generate non-trivial graphs with edges between modes belonging to different resonators, a beam splitter enacting a Hadamard transformation can be used, as in Figure 8 of the paper.

Next we show how Eq. (82) can be generated through squeezed bath engineering. Remarkably, the three criteria we have assumed for the graph G, that it is bicolorable and satisfies the two conditions listed above, are exactly the criteria first studied by Menicucci, Flammia and Pfister in Refs.[22,23] These authors showed that graphs satisfying these criteria corresponding to cluster states that are universal for quantum computing exists, and moreover how such cluster states can be prepared using a single optical parametric oscillator (OPO). Later, Wang and coworkers[24] presented an alternative implementation using a network of OPOs and beam splitters.

We adopt the scheme from Ref. 24 and use JTWPAs as squeezing sources in place of OPOs. The main difference between what we propose here and previous proposals is the dissipative nature of the interactions. While in Ref. 24 and previous work[22,23] the schemes were based on Hamiltonian interactions between internal cavity modes of OPOs, we are using dissipative interactions between resonator modes that are *external* to the squeezing sources. The CV modes of the cluster state never interact directly, but rather become entangled through absorption and stimulated emission of correlated photons from their environment. Even so, the graph constructions from Ref. 24 can be adopted almost directly for our purposes as well.

Following Ref. 24 the modes of the cluster states will be resonator modes with equally spaced frequencies $\omega_m = \omega_0 + m\Delta$, where ω_0 is some frequency offset and Δ the frequency separation. We require a number of degenerate modes for each frequency ω_m: to create a D-dimensional cluster state requires a $2 \times D$-fold degeneracy per frequency. Each mode is a vertex in the cluster state graph, and as will become clear below, a set of degenerate modes can be thought of as a graph "macronode".[24] It is convenient to relabel the frequencies ω_m with a "macronode index" $\mathcal{M} = (-1)^m m$.

A simple implementation is to embody the modes of the cluster state in $2 \times D$ identical multi-mode resonators. Each resonator is assumed to couple to a single squeezed bath, which we label by an index i. We use the same number of squeezing sources, and each source is pumped by a frequency $\Omega_i = \omega_0 + i\Delta/2$ where $i = m + n$ for some choice of frequencies $\omega_m \neq \omega_n$. The key to creating useful cluster states is to correlate the different baths by combining the output fields of broadband squeezing sources using interferometers.

We first consider the simplest situation where each resonator is coupled to the output field of a single squeezing source, as illustrated in Fig. 2 for $D = 1$. The output field of each squeezing source has correlation functions of the form given in Eq. (53)

$$\langle \hat{b}^\dagger_{j\omega} \hat{b}_{i\omega'} \rangle = \delta_{ji} N_j(\omega) \delta(\omega - \omega'), \tag{83a}$$

$$\langle \hat{b}_{j\omega} \hat{b}^\dagger_{i\omega'} \rangle = \delta_{ji} [N_j(\omega) + 1] \delta(\omega - \omega'), \tag{83b}$$

$$\langle \hat{b}_{j\omega} \hat{b}_{i\omega'} \rangle = i\delta_{ji} M_j(\omega) \delta(2\Omega_j - \omega - \omega'), \tag{83c}$$

where we assume that $M_j(\omega) > 0$ is real. With a JTPWA as a squeezing source, as long as the phase mismatch is small $\Delta k(\omega) \simeq 0$, the squeezing angle is frequency independent and $M(\omega)$ can thus be assumed real without loss of generality since any complex phase can be absorbed in a redefinition of the system operators $\hat{c}_v$. Using this in Eq. (66) and doing an RWA leaves us with the Lindbladian

$$\mathcal{L}_M = \sum_v \kappa_v \Big\{ (N_v + 1)\mathcal{D}[c_v] + N_v \mathcal{D}[c_v^\dagger] - \sum_{vw} \sqrt{\kappa_v \kappa_w} M_{vw} \mathcal{S}_i[c_v^\dagger, c_w^\dagger] \Big\}, \tag{84}$$

where we have labeled the resonator modes by a vertex index v, $N_v = N_j(\omega_v)$, with ω_v the frequency of mode v of the jth resonator, and the matrix M_{vw} is non-zero with value $M_{vw} = M_j(\omega_v)$ only if $\omega_v + \omega_w = 2\Omega_j$ and v and w both are associated to the jth resonator. This is of the form Eq. (82) if we assume equal decay rates, $\kappa_v \equiv \kappa$ and $N_v \equiv N$ and we write $M_{vw} = |M| a_{vw}$ with $|M| = \sqrt{N(N+1)}$ and $-1 \le a_{vw} \le 1$.

The graph generated by Eq. (84), defined by the adjacency matrix $A \sim M = [M_{vw}]$, is however not useful for measurement based quantum computing: it consists of a set of disjoint edges, as illustrated in Fig. 2 (c). Note that for the adjacency matrix of this graph to be self-inverse, $A = A^{-1}$, requires edges with weights $a_{vw} = 0, \pm 1$, meaning a flat, quantum limited squeezing spectrum such that $|M_j(\omega)| = |M_i(\omega')| = |M| = \sqrt{N(N+1)}$ within the relevant bandwidth. We assume in the following that $M(\omega) = M > 0$, such that the graph consists of a collection of identical two-mode cluster states with egdge weights $+1$.

Note that Eq. (84) can be brought into Lindblad form,

$$\mathcal{L}_M = \sum_v \mathcal{D}[L_v], \tag{85}$$

withLindblad operators

$$L_v = \cosh(r)\hat{a}_v + i\sinh(r) \sum_{w \in \mathcal{N}(v)} a_{vw} \hat{a}_w^\dagger, \tag{86}$$

where we have used that $A = A^{-1}$ and that we can write $N = \sinh(r)^2$, $M = \sinh(r)\cosh(r)$.

There are, of course, no edges between vertices associated to modes embodied in different resonators at this stage, as they interact with independent, uncorrelated baths. The key to generate non-trivial cluster states is to combine the output fields of the squeezing sources on beam splitters before being incident on the resonators, as illustrated for the $D = 1$ case in Figure 8 of the paper.

A general two-port beam splitter transformation for a pair of fields,

$$R_{ij}(\omega) = \begin{pmatrix} t_i(\omega) & r_i(\omega) \\ r_j(\omega) & t_j(\omega) \end{pmatrix}, \tag{87}$$

gives $\hat{b}_{i\omega} \to t_i(\omega)\hat{b}_{i\omega} + r_i(\omega)\hat{b}_{j\omega}$, where $t_i(\omega)$ and $r_i(\omega)$ are the transmittance and reflectance coefficients. The correlation functions in Eq. (83) thus transform to

$$\langle \hat{b}^\dagger_{j\omega} \hat{b}_{i\omega'} \rangle = \delta_{ij} N_j \delta(\omega - \omega'), \tag{88a}$$

$$\langle \hat{b}_{j\omega} \hat{b}^\dagger_{i\omega'} \rangle = \delta_{ij} (N_j + 1) \delta(\omega - \omega'), \tag{88b}$$

$$\begin{aligned} \langle \hat{b}_{j\omega} \hat{b}_{i\omega'} \rangle = {} & i t_j r_i M_j \delta(2\Omega_j - \omega - \omega') \\ & + i r_j t_i M_i \delta(2\Omega_i - \omega - \omega')]. \end{aligned} \tag{88c}$$

where we have suppressed the ω argument on the functions on the right hand side for notational simplicity, and used that unitarity of the beam splitter requires $t_j^* r_i + r_j^* t_i = 0$. We see that the form of the Lindbladian Eq. (82) is preserved, with a transformed squeezing matrix, $M = [M_{vw}] \to$

RMR^T, where $R = \bigoplus R_{ij}$ represents the beam splitter matrix R_{ij} acting on all pairs of degenerate modes belonging to resonators i and j.

Following Ref. 24 we take the beam splitter to be a Hadamard transformation

$$H = \frac{1}{\sqrt{2}} \begin{pmatrix} 1 & 1 \\ 1 & -1 \end{pmatrix}, \tag{89}$$

such that the squeezing matrix

$$M \to RMR^T, \tag{90}$$

where $R = \bigoplus H$ represents a Hadamard matrix acting on pairs of degenerate modes. Since $M \sim A$, the graph of course transforms in the same way. For the $D = 1$ case this gives the graph illustrated in Figure 8 of the paper. Note that the transformed adjacency matrix RAR^T is still self-inverse since R is orthogonal.[24]

This can be generalized in a straight forward manner to combine multiple squeezing sources. For $2 \times D$ sources, we can construct a $2D \times 2D$ Hadamard matrix by composing together 2×2 Hadamard matrices, $H_D = H^{\otimes D}$.[24] In practice this is done by combining the output fields pairwise on two-port beam splitters in a cascaded fashion, as illustrated for the case $D = 2$ in Figure 9 of the paper, and explained in more detail in Ref. 24. The total transformation on the squeezing matrix is $R = \bigoplus_{\mathcal{M}} H_D$, representing a $2D \times 2D$ Hadamard transformation on each *macronode* $\mathcal{M}$, *i.e.*, each set of $2 \times D$ degenerate modes.

As shown in Ref. 24, graphs defined by the adjacency matrix $A \sim M$ corresponding to D-dimensional cluster states can be generated in this way, where in particular the $D = 2$ case is universal for measurement based quantum computing.

References

[1] Devoret, M. H. Quantum fluctuations in electrical circuits. *Les Houches Lecture Notes* (1995).

[2] Bhat, N. A. R. & Sipe, J. E. Hamiltonian treatment of the electromagnetic field in dispersive and absorptive structured media. *Phys. Rev. A* **73**, 063808 (2006).

[3] Drummond, P. D. & Hillery, M. *The quantum theory of nonlinear optics* (Cambridge University Press, 2014).

[4] Santos, D. J. & Loudon, R. Electromagnetic-field quantization in inhomogeneous and dispersive one-dimensional systems. *Phys. Rev. A* **52**, 1538–1549 (1995).

[5] Nigg, S. E. *et al.* Black-box superconducting circuit quantization. *Physical review letters* **108**, 240502 (2012).

[6] Hopfield, J. Theory of the contribution of excitons to the complex dielectric constant of crystals. *Physical Review* **112**, 1555 (1958).

[7] Huttner, B., Baumberg, J. & Barnett, S. Canonical quantization of light in a linear dielectric. *EPL (Europhysics Letters)* **16**, 177 (1991).

[8] Huttner, B. & Barnett, S. M. Quantization of the electromagnetic field in dielectrics. *Phys. Rev. A* **46**, 4306–4322 (1992).

[9] Yaakobi, O., Friedland, L., Macklin, C. & Siddiqi, I. Parametric amplification in josephson junction embedded transmission lines. *Phys. Rev. B* **87**, 144301 (2013).

[10] O'Brien, K., Macklin, C., Siddiqi, I. & Zhang, X. Resonant phase matching of josephson junction traveling wave parametric amplifiers. *Phys. Rev. Lett.* **113**, 157001 (2014).

[11] White, T. *et al.* Traveling wave parametric amplifier with josephson junctions using minimal resonator phase matching. *Applied Physics Letters* **106**, 242601 (2015).

[12] Eichler, C. *et al.* Observation of two-mode squeezing in the microwave frequency domain. *Phys. Rev. Lett.* **107**, 113601 (2011).

[13] Flurin, E., Roch, N., Mallet, F., Devoret, M. H. & Huard, B. Generating entangled microwave radiation over two transmission lines. *Phys. Rev. Lett.* **109**, 183901 (2012).

[14] Eichler, C., Salathe, Y., Mlynek, J., Schmidt, S. & Wallraff, A. Quantum-limited amplification and entanglement in coupled nonlinear resonators. *Phys. Rev. Lett.* **113**, 110502 (2014).

[15] Forgues, J.-C., Lupien, C. & Reulet, B. Experimental violation of bell-like inequalities by electronic shot noise. *Phys. Rev. Lett.* **114**, 130403 (2015).

[16] Grimsmo, A. L., Qassemi, F., Reulet, B. & Blais, A. Quantum optics theory of electronic noise in coherent conductors. *Phys. Rev. Lett.* **116**, 043602 (2016).

[17] Clerk, A. A., Devoret, M. H., Girvin, S. M., Marquardt, F. & Schoelkopf, R. J. Introduction to quantum noise, measurement, and amplification. *Reviews of Modern Physics* **82**, 1155 (2010).

[18] Carmichael, H. J. Quantum trajectory theory for cascaded open systems. *Phys. Rev. Lett.* **70**, 2273–2276 (1993).

[19] Gardiner, C. W. Driving a quantum system with the output field from another driven quantum system. *Phys. Rev. Lett.* **70**, 2269–2272 (1993).

[20] Gardiner, C. & Zoller, P. *Quantum Noise: A Handbook of Markovian and Non-Markovian Quantum Stochastic Methods with Applications to Quantum Optics* (Springer, New York, 2004).

[21] Koga, K. & Yamamoto, N. Dissipation-induced pure gaussian state. *Physical Review A* **85**, 022103 (2012).

[22] Flammia, S. T., Menicucci, N. C. & Pfister, O. The optical frequency comb as a one-way quantum computer. *Journal of Physics B: Atomic, Molecular and Optical Physics* **42**, 114009 (2009).

[23] Menicucci, N. C., Flammia, S. T. & Pfister, O. One-way quantum computing in the optical frequency comb. *Phys. Rev. Lett.* **101**, 130501 (2008).

[24] Wang, P., Chen, M., Menicucci, N. C. & Pfister, O. Weaving quantum optical frequency combs into continuous-variable hypercubic cluster states. *Phys. Rev. A* **90**, 032325 (2014).